Cavitating Cascades

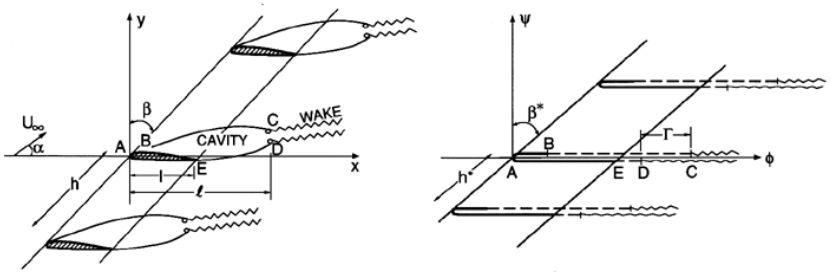

Figure 1: On the left is the physical plane (z-plane), and on the right is the complex potential plane (f-plane) for the planar flow through a cascade of cavitating hydrofoils. The example shown is for supercavitating foils. For partial cavitation the points D and E merge and the point C is on the upper wetted surface of the foil. For a sharp leading edge the points A and B merge. Figures adapted from Furuya (1975a).

Because cavitation problems are commonly encountered in liquid turbomachines (pumps, turbines) and on propellers, the performance of a cascade of hydrofoils under cavitating conditions is of considerable practical importance. A typical cascade geometry (z-plane) is shown on the left in Figure 1; in the terminology of these flows the angle, β, is known as the "stagger angle" and $1/h$, the ratio of the blade chord to the distance between the blade tips, is known as the "solidity." The corresponding complex potential plane (f-plane) is shown on the right. Note that the geometry of the linearized physical plane is very similar to that of the f-plane.

The first step in the analysis of the planar potential flow in a cascade (whether by linear or nonlinear methods) is to map the infinite array of blades in the f-plane (or the linearized z-plane) into a ζ-plane in which there is a single wetted surface boundary and a single cavity surface boundary. This is accomplished by the well-known cascade mapping function

$$f \quad \text{or} \quad z = \frac{h}{2\pi}\left[e^{-i\beta}\ln(1-\zeta/\zeta_H) + e^{i\beta}\ln(1-\zeta/\bar{\zeta}_H)\right] \tag{Nui1}$$

where h^* (or h) is the distance between the leading edges of the blades and β^* (or β) is the stagger angle of the cascade in the f-plane (or the linearized z-plane). This mapping produces the ζ-plane shown in

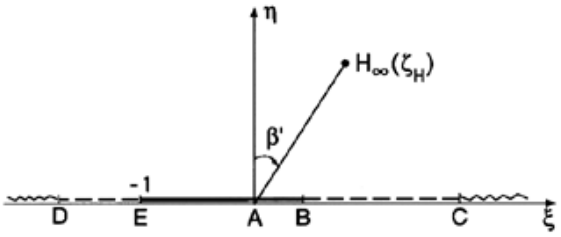

Figure 2: The ζ-plane obtained by using the cascade mapping function.

Figure 2 where H_∞ ($\zeta = \zeta_H$) is the point at infinity in the original plane and the angle β' is equal to the

stagger angle in the original plane. The solution is obtained when the mapping $w(\zeta)$ has been determined and all the boundary conditions have been applied.

For a supercavitating cascade, a nonlinear solution was first obtained by Woods and Buxton (1966) for the case of a cascade of flat plates. Furuya (1975a) expanded this work to include foils of arbitrary geometry. An interesting innovation introduced by Woods and Buxton was the use of Tulin's (1964) double-spiral-vortex model for cavity closure, but with the additional condition that the difference in the velocity potentials at the points C and D (Figure 1) should be equal to the circulation around the foil.

Linear theories for a cascade began much earlier with the work of Betz and Petersohn (1931), who solved the problem of infinitely long, open cavities produced by a cascade of flat plate hydrofoils. Sutherland and Cohen (1958) generalized this to the case of finite supercavities behind a flat plate cascade, and Acosta (1960) solved the same problem but with a cascade of circular-arc hydrofoils. Other early contributions to linear cascade theory for supercavitating foils include the models of Duller (1966) and Hsu (1972) and the inclusion of the effect of rounded leading edges by Furuya (1974).

Cavities initiated at the leading edge are more likely to extend beyond the trailing edge when the solidity and the stagger angle are small. Such cascade geometries are more characteristic of propellers and, therefore, the supercavitating cascade results are more often utilized in that context. On the other hand, most cavitating pumps have larger solidities (> 1) and large stagger angles. Consequently, partial cavitation is the more characteristic condition in pumps, particularly since the pressure rise through the pump is likely to collapse the cavity before it emerges from the blade passage. Partially cavitating cascade analysis began with the work of Acosta and Hollander (1959), who obtained the linear solution for a cascade of infinitely long flat plates, the geometry of which is shown in Figure 3. The appropriate cascade mapping is then the

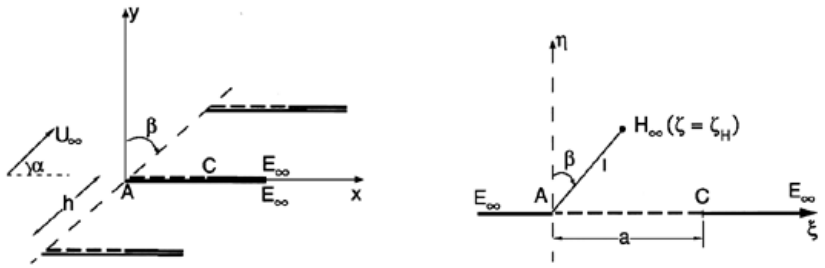

Figure 3: The linearized z-plane (left) and the ζ-plane (right) for the linear solution of partial cavitation in an infinitely long cascade of flat plates (Acosta and Hollander 1959). The points E_∞ and H_∞ are respectively the points at upstream and downstream infinity in the z-plane.

version of Equation (**??**) with z on the left-hand side. The Acosta and Hollander solution is algebraically simple and therefore makes a good, specific example. The length of the cavity in the ζ-plane, a, provides a convenient parameter for the problem and should not be confused with the actual cavity length, ℓ. Given the square-root singularities at A and C, the complex velocity, $w(\zeta)$, takes the form

$$\frac{w(\zeta)}{U_\infty} = (1+\sigma)^{\frac{1}{2}} + C_1 \left[\frac{\zeta}{\zeta - a}\right]^{\frac{1}{2}} - C_2 \left[\frac{\zeta - a}{\zeta}\right]^{\frac{1}{2}} \tag{Nui2}$$

where the real constants, C_1 and C_2, must be determined by the conditions at upstream and downstream infinity. As $x \to -\infty$ or $\zeta \to \zeta_H = ie^{-i\beta}$ we must have $w/U_\infty = e^{-i\alpha}$ and therefore

$$C_1 \left[\frac{\zeta_H}{\zeta_H - a}\right]^{\frac{1}{2}} - C_2 \left[\frac{\zeta_H - a}{\zeta_H}\right]^{\frac{1}{2}} + (1+\sigma)^{\frac{1}{2}} = e^{-i\alpha} \tag{Nui3}$$

and, as $x \to +\infty$ or $|\zeta| \to \infty$, continuity requires that

$$C_1 - C_2 + (1+\sigma)^{\frac{1}{2}} = \cos(\alpha+\beta) \big/ \cos(\beta) \tag{Nui4}$$

The complex equation (Nui3) and the scalar equation (Nui4) permit evaluation of C_1, C_2, and a in terms of the parameters of the physical problem, σ and β. Then the completed solution can be used to evaluate such features as the cavity length, ℓ:

$$\frac{\ell}{h} = \frac{1}{\pi} Re\left\{e^{-i\beta} \ln\left(1 + iae^{i\beta}\right)\right\} \tag{Nui5}$$

Wade (1967) extended this partial cavitation analysis to cover flat plate foils of finite length, and Stripling and Acosta (1962) considered the nonlinear problem. Brennen and Acosta (1973) presented a simple, approximate method by which a finite blade thickness can be incorporated into the analysis of Acosta and Hollander. This is particularly valuable because the choked cavitation number, σ_c, is quite sensitive to the blade thickness or radius of curvature of the leading edge. The following is the expression for σ_c from the Brennen and Acosta analysis:

$$\sigma_c = \left[1 + 2\sin\frac{\alpha}{2}\sec\left(\frac{\pi}{4} - \frac{\beta}{2}\right)\sin\left(\frac{\pi}{4} - \frac{\beta}{2} - \frac{\alpha}{2}\right) + 2d\sin^2\left(\frac{\pi}{4} - \frac{\beta}{2}\right)\right]^{\frac{1}{2}} - 1 \tag{Nui6}$$

where d is the ratio of the blade thickness to normal blade spacing, $h\cos\beta$, far downstream. Since the validity of the linear theory requires that $\alpha \ll 1$ and since many pumps (for example, cavitating inducers) have stagger angles close to $\pi/2$, a reasonable approximation to equation (Nui6) is

$$\sigma_c \approx \alpha(\theta - \alpha) + \theta^2 d \tag{Nui7}$$

where $\theta = \pi/2 - \beta$. This limit is often used to estimate the breakdown cavitation number for a pump based on the heuristic argument that long partial cavities that reach the pump discharge would permit substantial deviation angles and therefore lead to a marked decline in pump performance (Brennen and Acosta 1973).

Note, however, that under the conditions of an inviscid model, a small partial cavity will not significantly alter the performance of the cascade of higher solidity (say, $1/h > 1$) since the discharge, with or without the cavity, is essentially constrained to follow the direction of the blades. On the other hand, the direction of flow downstream of a supercavitating cascade will be significantly affected by the cavities, and the corresponding lift and drag coefficients will be altered by the cavitation. We return to the subject of supercavitating cascades to demonstrate this effect.

A substantial body of data on the performance of cavitating cascades has been accumulated through the efforts of Numachi (1961, 1964), Wade and Acosta (1967), and others. This allows comparison with the analytical models, in particular the supercavitating theories. Figure 4 provides such a comparison between measured lift and drag coefficients (defined as normal and parallel to the direction of the incident stream) for a particular cascade and the theoretical results from the supercavitating theories of Furuya (1975a) and Duller (1966). Note that the measured lift coefficients exhibit a rapid decline in cascade performance as the cavitation number is reduced and the supercavities grow. However, it is important to observe that this degradation does not occur until the cavitation is quite extensive. The cavitation inception numbers for the experiments were $\sigma_i = 2.35$ (for 8°) and $\sigma_i = 1.77$ (for 9°). However, the cavitation number must be lowered to about 0.5 before the performance is adversely affected. In the range of σ in between are the partial cavitation states for which the performance is little changed.

For the cascades and incidence angles used in the example of Figure 4, Furuya (1975a) shows that the linear and nonlinear supercavitation theories yield results that are similar and close to those of the experiments.

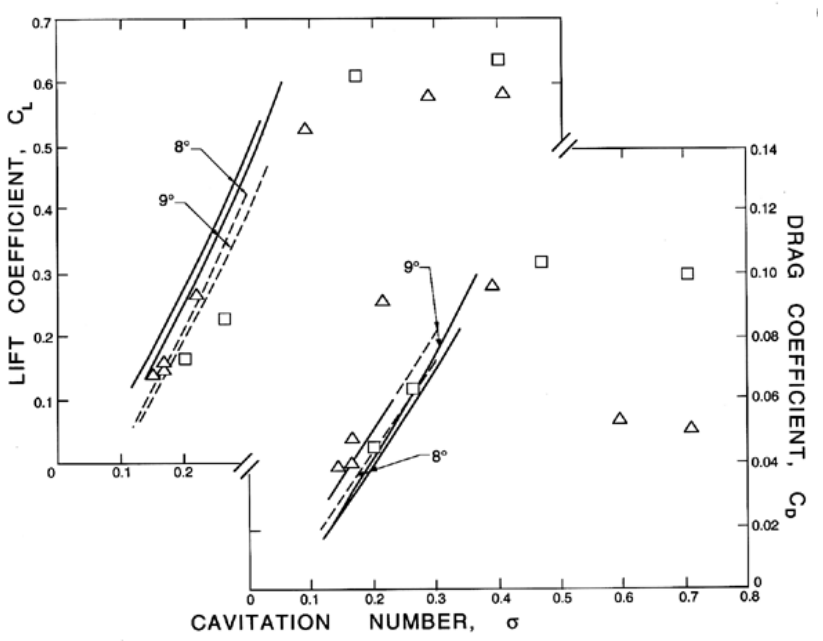

Figure 4: Lift and drag coefficients as functions of the cavitation number for cascades of solidity, 0.625, and stagger angle, $\beta = 45° - \alpha$, operating at angles of incidence, α, of 8° (△) and 9° (□). The points are from the experiments of Wade and Acosta (1967), and the analytical results for a supercavitating cascade are from the linear theory of Duller (1966) (dashed lines) and the nonlinear theory of Furuya (1975a) (solid lines).

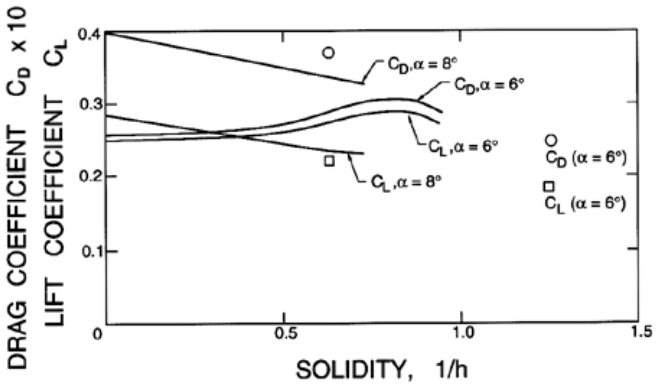

Figure 5: Lift and drag coefficients as functions of the solidity for cascades of stagger angle, $\beta = 45° - \alpha$, operating at the indicated angles of incidence, α, and at a cavitation number, $\sigma = 0.18$. The points are from the experiments of Wade and Acosta (1967), and the lines are from the nonlinear theory of Furuya (1975). Reproduced from Furuya (1975a).

This is illustrated in Figure 4. However, Furuya also demonstrates that there are circumstances in which the linear theories can be substantially in error and for which the nonlinear results are clearly needed. The effect of the solidity, $1/h$, on the results is also important because it is a major design factor in determining the number of blades in a pump or propeller. Figure 5 illustrates the effect of solidity when large supercavities are present ($\sigma = 0.18$). Note that the solidity has remarkably little effect.